

## DETERMINATION OF THE FIRING ANGLE FOR A DYNAMIC FAULT CURRENT LIMITER (DFCL) IN CASE WITHOUT A FAULT

Hubert Rubenbauer, Gerhard Herold  
 Institute of Electrical Power Systems of the University Erlangen-Nuremberg  
 Cauerstrasse 4 - Building 1, D-91058 Erlangen  
 Germany  
 rubenbauer@eev.eei.uni-erlangen.de, herold@eev.eei.uni-erlangen.de

### ABSTRACT

In faultless operation mode it is very important, that the investigated Dynamic Fault Current Limiter (DFCL) has got only little influence on the protected electrical network. Since the DFCL is based on a thyristor rectifier, this nearly uninfluenced operation is ensured by an appropriate firing angle. To determine this certain firing angle in this paper a numerical method is described, which is derived from the different circuit states. Besides the determination of the right DFCL control in faultless operation mode, one understands the dependence of the operation ranges of the DFCL on the impedance ratio of the surrounding network. Altogether this knowledge is very important to design a control system for a fast and secure DFCL operation in case without a fault.

### KEY WORDS

Power electronics, power system protection, FCL

### 1. Introduction

In [1] (and partly in [2]) a highly flexible Fault Current Limiter (FCL) is presented and its different operation modes are described. This so-called Dynamic Fault Current Limiter (DFCL) is installed directly in a transformers neutral point as shown in Fig. 1.

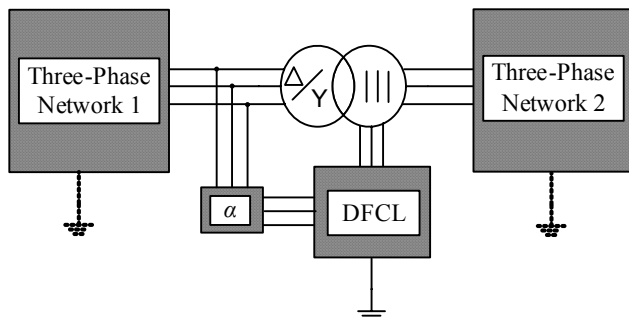


Fig. 1: Place of installation of the DFCL and reference voltages for the firing angle  $\alpha$

In this case fault currents in Three-Phase Network 2, which are supplied from Three-Phase Network 1, are limited by the DFCL. Since the DFCL is based on a six-pulse thyristor rectifier, reference voltages must be chosen to control the firing pulses according to the firing

angle  $\alpha$ . Herein the line-to-line voltages directly on the transformer are selected (voltage side with the neutral point in wye or delta connection, see Fig. 1). The three-phase networks in Fig. 1 can be grounded as it is adumbrated by dashed lines, because the DFCL is also able to handle grounded faults as described in [1].

The general circuit diagram of the DFCL is depicted in Fig. 2. It consists of a six-pulse thyristor rectifier (T1 to T6), an additional thyristor arm (T7 and T8), a freewheeling diode and a limiting coil (represented by  $R_d$  and  $L_d$ ) on the d.c. side. By using the DFCL it is possible to handle all types of faults in three different ways [1]. On the one hand by blocking the thyristors' firing pulses the short circuit current can be switched off in about 12ms, which leads to only little mechanical and thermal stress by the short-circuit. On the other hand the DFCL may be controlled in such a way, that the fault current can flow nearly unaffected. Furthermore after the transient oscillations by changing the firing angle it is possible to adjust the maximum value of the fault current between zero and its steady short-circuit current. In general the surge short-circuit current is suppressed by the limiting coil on the d.c. side.

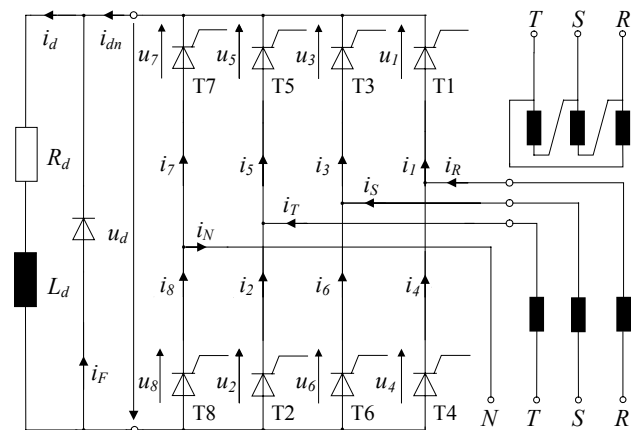


Fig. 2: Dynamic Fault Current Limiter (DFCL) connected to a Diii-transformer

But the matter of this paper is not the investigation of the behaviour of the DFCL in fault case. The attention is directed to the stationary operation of the DFCL in case

without a fault, to get an idea how its operation range depends on the whole system structure. In the following considerations symmetrical behaviour of the whole power system is assumed. Therefore the thyristor branch with T7 and T8, which is necessary within the DFCL to handle all grounded operations, can be disregarded (see simplification under point 2.).

An important general FCL's characteristic is that the current limiting device should have only little influence on the surrounding system in faultless case - the FCL should be like 'not present'. To provide this the DFCL must operate in a way that always three thyristors of the six-pulse rectifier (T1 to T6) lead current, because otherwise one of the three-phase currents is interrupted and the protected network, Three-Phase-Network 2, is heavily affected. So the DFCL must work like a diode rectifier with a parallel freewheeling arm, to have nearly no influence.

If a symmetrical operation of the electrical power system is considered, typical runs of the three phase currents  $i_R$ ,  $i_S$  and  $i_T$  besides the d.c. currents  $i_d$  and  $i_{dn}$  can be seen in Fig. 3. Thereby all currents are referenced to the peak value of the three-phase currents, which would flow, if no DFCL is integrated in the system. Furthermore the time axes are referenced to angular frequency  $\omega$ . Within Fig. 3 no phase current is interrupted and  $i_d$  or  $i_{dn}$  respectively is equal to the maximum absolute value of the three-phase currents. In Fig. 4 only the associated d.c. currents  $i_d$ ,  $i_{dn}$  and  $i_F$  at symmetrical system behaviour are depicted. The d.c. period, during which thyristors T1, T2 and T3 are conductive, is grey shaded both in Fig. 3 and in Fig. 4.

In order that all three-phase currents  $i_R$ ,  $i_S$  and  $i_T$  in Fig. 2 can flow uninterrupted through Three-Phase-Network 2 (see Fig. 1), it is necessary, that always three thyristor valves of the six-pulse rectifier lead current. If for example thyristors T1, T2 and T3 are conductive,  $i_R$  and  $i_S$  add up to the d.c. current  $i_{dn}$ , which is equal to  $i_d$  in case of a blocking freewheeling diode with  $i_F = 0$  (see Fig. 4). The d.c. current  $i_{dn}$  is also equal to  $-i_T$  and flows back into the three-phase system. If otherwise thyristors T2 to T4 conduct, the d.c. sided current  $i_{dn}$  is composed of  $-i_R$  and  $-i_T$  or is equal to  $i_S$  respectively. But if with T2 and T3 only two thyristors are conductive,  $i_{dn}$  is equal to  $i_S$  and  $-i_T$  and phase current  $i_R$  is interrupted. The last case is undesirable in faultless operation mode.

Altogether in the case, when always three thyristor values lead current, according to Fig. 3 the three phase currents  $i_R$ ,  $i_S$  and  $i_T$  are only zero in their natural zero crossing. Then for the protected three-phase network the DFCL behaves more or less like an impedance afflicted neutral point. During a blocking freewheeling diode this impedance is relatively high, because all three phase currents  $i_R$ ,  $i_S$  and  $i_T$  have to flow through the limiting element ( $R_d$ ,  $L_d$ ). In case of a current leading freewheeling arm the limiting coil is decoupled from the a.c. side and the impedance of the neutral point is relatively low.

Furthermore Fig. 3 shows clearly the six-pulse character of the DFCL, because one can identify six d.c.

periods during the depicted a.c. period. In Fig. 4 one can recognize, that at the beginning of such a stationary d.c. period the freewheeling diode is conducting. After a short period of time the diode leads current till the end of the d.c. period. Altogether Fig. 3 and Fig. 4 present the desired operation mode of the DFCL in case without a fault. This is the matter of investigation in this paper.

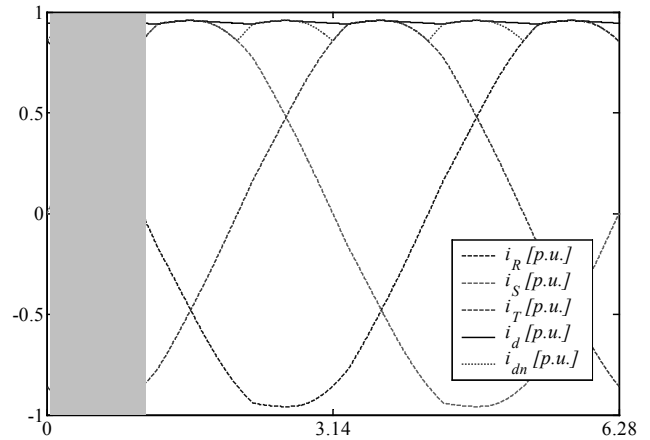


Fig. 3: Three-phase currents  $i_R$ ,  $i_S$  and  $i_T$  and d.c. currents  $i_d$  and  $i_{dn}$  at symmetrical system behaviour

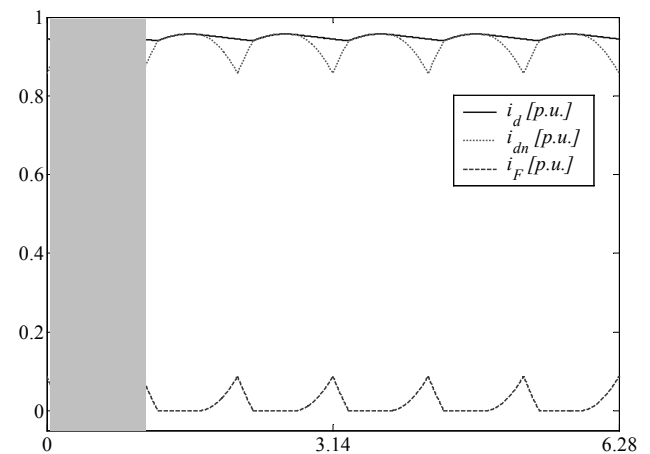


Fig. 4: D.C. currents  $i_d$ ,  $i_{dn}$  and  $i_F$  at symmetrical system behaviour

To analyse the faultless operation mode, symmetrical system behaviour is assumed below and the general system with DFCL is simplified to a clearly arranged network. Therefore grounded system operations are not considered. In the following this assumptions will be used to find out the DFCL's firing angle  $\alpha$ , which is necessary for the steady faultless operation mode with always three conductive thyristor valves. By considering different impedance ratios of the three-phase network one gets an idea how the firing angle  $\alpha$  has to be adapted, if the network state changes by additional or switched off elements. This is very valuable information to build up a fast and save control of the DFCL.

## 2. Simplification of the system

If Three-Phase Network 1 in Fig. 1 is considered to be a stiff system with infinitely small system impedance, it can be modelled by just a three-phase voltage source ( $u_{sR}$ ,  $u_{sS}$  and  $u_{sT}$ ) as shown in Fig. 5. Further the Three-Phase Network 2 is supposed without sources and is just represented by its symmetrical system impedance ( $R_L$ ,  $L_L$ ) within Fig. 5.

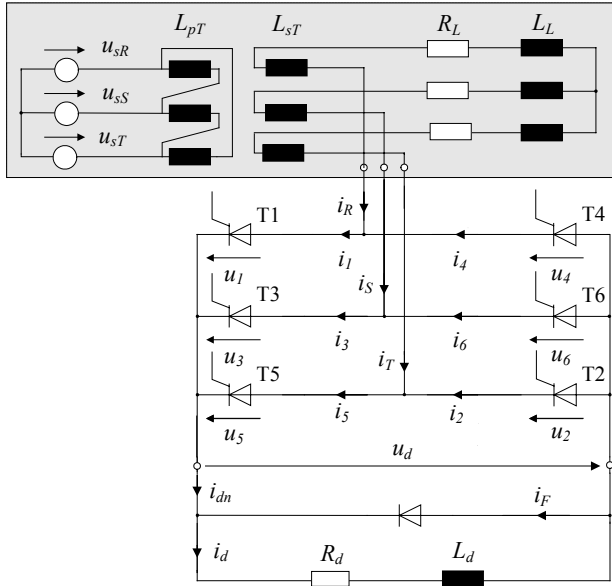


Fig. 5: Analysed sample system

Moreover the fourth thyristor branch, which is in Fig. 2 parallel to the six-pulse rectifier and consists of T7 and T8, is neglected in Fig. 5. This is allowed, because this thyristor branch handles grounded system operation modes, which do not have to be considered at ideal symmetrical system behaviour. The shaped area in Fig. 5 can be subsumed and simplified to the shaped area in Fig. 6 by using Thevenin's Theorem. Thereby the whole three-phase network is represented by its open-circuit voltages  $u_{pR}$ ,  $u_{pS}$  and  $u_{pT}$  and its system impedance ( $R_k$ ,  $X_k$ ), which contains  $R_L$ ,  $X_L = \omega L_L$ ,  $X_{pT} = \omega L_{pT}$  and  $X_{sT} = \omega L_{sT}$ .

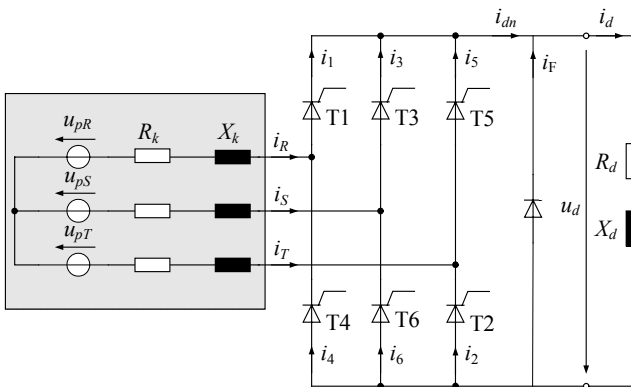


Fig. 6: Simplified, investigated system

In the system in Fig. 5 the reference voltages of the firing angle  $\alpha_0$  are the line-to-line voltages  $u_{sRS} = u_{sR} - u_{sS}$ ,  $u_{sST} = u_{sS} - u_{sT}$  and  $u_{sTR} = u_{sT} - u_{sR}$  directly at the transformer.

By the transition from the structure in Fig. 5 to that in Fig. 6 one has to take the phase displacement between the reference voltages and the thyristor rectifier into consideration. On the one hand in Fig. 5 between the Three-Phase-Network 2 and the reference voltages is a Diii-transformer, which leads to a phase rotation of  $150^\circ$ . On the other hand the installation of the DFCL in the transformer's neutral point has to be considered with a phase displacement of  $180^\circ$ .

For the arrangement in Fig. 6, wherein the line-to-line voltages  $u_{pRS} = u_{pR} - u_{pS}$ ,  $u_{pST} = u_{pS} - u_{pT}$  and  $u_{pTR} = u_{pT} - u_{pR}$  directly at the voltage sources are used as reference for the firing angle  $\alpha$ , the following correlation exists between  $\alpha$  and the original firing angle  $\alpha_0$

$$\alpha_0 = \alpha + 150^\circ - 180^\circ = \alpha - 30^\circ \quad (1)$$

All in all the general system in Fig. 1 is now simplified to the circuit diagram in Fig. 6, which is analysed in the following. Of course the resulting system is a simple three-phase system connected to an inductive loaded six-pulse thyristor rectifier with an additional freewheeling diode (B6F-circuit). The big difference to conventional considerations regarding this system structure is that in Fig. 6 the values of the resistance  $R_k$  and the reactance  $X_k$  can change. In usual applications with thyristor rectifiers it can be assumed that  $R_k$  and  $X_k$  consist only of the impedance of the converter transformer, which is mainly inductive. Thus  $R_k$  and  $X_k$  can be seen as nearly constant.

In the case, which is investigated in this paper, on the one hand  $R_k$  and  $X_k$  contain the impedance of the converter transformer, which is supposed to be purely inductive ( $X_{pT}$ ,  $X_{sT}$ ). On the other hand they include also the system impedance ( $R_L$ ,  $X_L$ ) of the protected network. So if the system impedance changes by switching actions, system processes or a fault occurrence, also  $R_k$  and  $X_k$  change their values. By this impedance variation also the firing angle  $\alpha$  has to be adapted to guarantee a certain operation mode.

In the next section a numerical analysing method is described to get an idea about the correlation between the firing angle  $\alpha$  and the impedance ratio of  $R_k$  and  $X_k$ .

## 3. Numerical determination of the firing angle $\alpha$

The following analysis of the DFCL is based on the different circuit states, which can appear during the DFCL operation in case without a fault. During a state space analysis the differential equations for all considered states are set up and the transition conditions are formulated. At a certain firing angle  $\alpha$  the steady state of the system is calculated and compared with the desired state. If the

resulting state is not equal to the aspired one, the firing angle  $\alpha$  is changed till the desired state is reached.

During the DFCL operation in case without a fault always three thyristors must lead current as described above and depicted in Fig. 3. In stationary state it is supposed that the freewheeling diode blocks and fires during a d.c. period like in Fig. 4. So the desired state consists of two circuit states:

- three conducting thyristor valves at a blocking freewheeling diode (abbr.: 3V)
- three conductive thyristors with a conducting freewheeling diode (abbr.: 3VF)

This is reached at exactly one firing angle  $\alpha_3$ . If on the one hand the firing angle is greater than  $\alpha_3$ , during the d.c. period also the states will appear, in which only two thyristors lead current. So one get those additional circuit states:

- two conducting thyristor valves at a blocking freewheeling diode (abbr.: 2V)
- two conductive thyristors with a conducting freewheeling diode (abbr.: 2VF)

On the other hand, if the firing angle is smaller than  $\alpha_3$ , four thyristors would lead current and short-circuit the thyristor bridge. This circuit state can be treated like the short-circuit by the freewheeling diode. Therefore it is possible to describe this situation with the 3VF-state.

In addition four states (3VF, 3V, 2VF and 2V) are enough to describe the system behaviour at and nearby the steady state of the DFCL in case without a fault in the protected system.

For the description of these four states in the system with a six-pulse thyristor rectifier and freewheeling diode (see Fig. 6) the transformation to space phasors and zero components is used. The space phasor is generally given by

$$\underline{v} = \frac{2}{3}(v_R + \underline{a} \cdot v_S + \underline{a}^2 \cdot v_T) \quad (2)$$

and the associated zero component by

$$v_0 = \frac{1}{3}(v_R + v_S + v_T) \quad (3)$$

Therein the rotating operator  $\underline{a}$  is defined by

$$\underline{a} = e^{j\frac{2}{3}\pi} \quad (4)$$

Because of the periodical behaviour of a six-pulse thyristor bridge it is enough, to analyse only one d.c. period, which is a sixth of the a.c. period. Herein for the state with three conducting thyristors the d.c. period is considered, in which thyristors T1, T2 and T3 are conductive (see shaped areas in Fig. 3 and Fig. 4). In the case of only two conducting thyristors the circuit state with current leading thyristors T2 and T3 is investigated. In the style of [3] the four states can be described as follows:

- 3V: only three thyristors (T1, T2, T3)

The space phasor of the three-phase currents  $i_R, i_S$  and  $i_T$  is equal to

$$\underline{i} = \frac{2}{3}(i_R + \underline{a} \cdot i_S + \underline{a}^2 \cdot i_T) = \frac{2}{3}(1 - \underline{a})i_{k,3V} - \underline{a}^2 i_{dn,3V} \quad (5)$$

The currents  $i_{k,3V}$  and  $i_{dn,3V}$  can be calculated by using the circuit diagrams in Fig. 7 or Fig. 8 respectively.

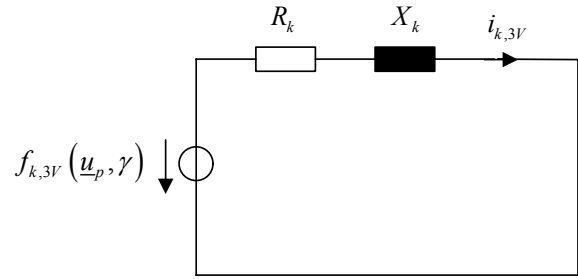


Fig. 7: State 3V and 3VF: commutation current  $i_{k,3V}$

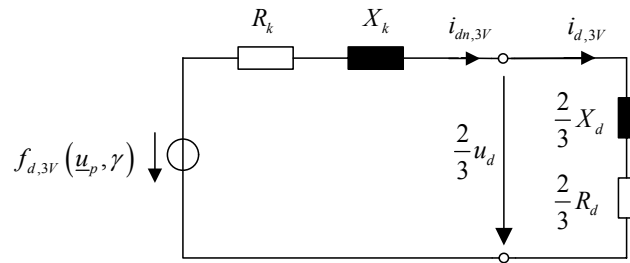


Fig. 8: State 3V: d.c. currents  $i_{dn,3V}$  or  $i_{d,3V}$  respectively

Thereby the voltage sources are

$$f_{k,3V}(\underline{u}_p, \gamma) = \frac{\sqrt{3}}{2} \hat{U}_p \cdot \cos(\omega t + \gamma + \frac{\pi}{6}) \quad (6)$$

and

$$f_{d,3V}(\underline{u}_p, \gamma) = \hat{U}_p \cdot \cos(\omega t + \gamma - \frac{\pi}{3}) \quad (7)$$

The resulting currents  $i_{k,3V}$  and  $i_{dn,3V}$  consist of stationary and transient parts

$$i_{k,3V} = c_{k,3V} \cdot e^{p_k \cdot \omega t} + i_{k,3V,w} \quad (8)$$

$$i_{dn,3V} = c_{dn,3V} \cdot e^{p_{dn,3V} \cdot \omega t} + i_{dn,3V,w} \quad (9)$$

- 2V: only two thyristors (T2, T3)

The space phasor of the three-phase currents is

$$\underline{i} = \frac{2}{3}(\underline{a} - \underline{a}^2)i_{d,2V} \quad (10)$$

The current  $i_{d,2V}$  can be calculated by using the circuit diagram depicted in Fig. 9. Thereby the voltage source is

$$f_{d,2V}(\underline{u}_p, \gamma) = \frac{\sqrt{3}}{2} \hat{U}_p \cdot \cos(\omega t + \gamma - \frac{\pi}{2}) \quad (11)$$

The current  $i_{dn,2V}$  results also from a differential equation as

$$i_{dn,2V} = c_{dn,2V} \cdot e^{p_{dn,2V} \cdot \omega t} + i_{dn,2V,w} \quad (12)$$

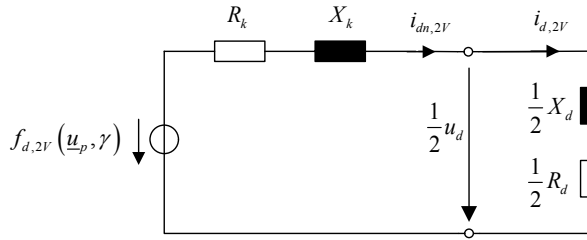


Fig. 9: State 2V: d.c. currents  $i_{dn,2V}$  or  $i_{d,2V}$  respectively

In the states with a conductive freewheeling diode the freewheeling arm is represented by the diode's threshold voltage  $U_0$  and the complete resistance  $R_F$  of the freewheeling arm.

- 3VF: three thyristors ( $T1, T2, T3$ ) and freewheeling diode

The space phasor of the three-phase currents is

$$\underline{i} = \frac{2}{3}(1-a)i_{k,3V} - \underline{a}^2 i_{dn,3VF} \quad (13)$$

The currents  $i_{k,3V}$  and  $i_{dn,3VF}$  can be calculated by using the circuit diagrams in Fig. 7 or Fig. 10 respectively.

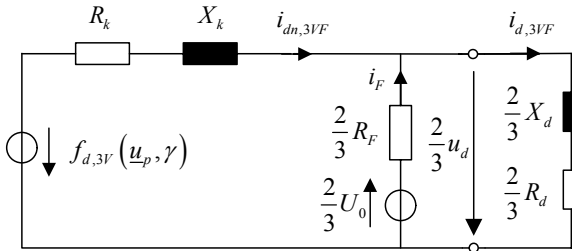


Fig. 10: State 3VF: d.c. currents  $i_{dn,3VF}$  or  $i_{d,3VF}$  respectively

The voltage source is given by equation (7). The resulting current  $i_{k,3V}$  is like in equation (8) and also currents  $i_{dn,3VF}$  and  $i_{d,3VF}$  consist of stationary and transient parts

$$i_{dn,3VF} = c_{dn,3VF,1} \cdot e^{p_1 \cdot \omega t} + c_{dn,3VF,2} \cdot e^{p_2 \cdot \omega t} + i_{dn,3VF,g} + i_{dn,3VF,w} \quad (14)$$

$$i_{d,3VF} = c_{d,3VF,1} \cdot e^{p_1 \cdot \omega t} + c_{d,3VF,2} \cdot e^{p_2 \cdot \omega t} + i_{d,3VF,g} + i_{d,3VF,w} \quad (15)$$

- 2VF: two thyristors ( $T2, T3$ ) and freewheeling diode

The space phasor of the three-phase currents is

$$\underline{i} = \frac{2}{3}(\underline{a} - \underline{a}^2) i_{d,2VF} \quad (16)$$

The currents  $i_{d,2VF}$  can be calculated by using the circuit diagram depicted in Fig. 11

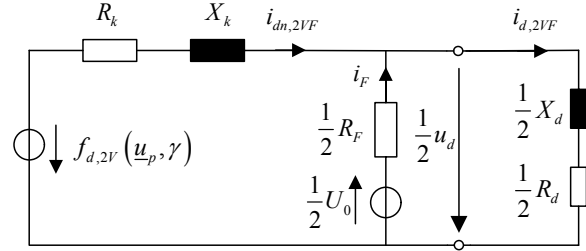


Fig. 11: State 2VF: d.c. currents  $i_{dn,2VF}$  or  $i_{d,2VF}$  respectively

The voltage source is given by equation (9). The currents  $i_{dn,2VF}$  or  $i_{d,2VF}$  respectively again consists of two transient and two stationary parts

$$i_{dn,2VF} = c_{dn,2VF,1} \cdot e^{p_1 \cdot \omega t} + c_{dn,2VF,2} \cdot e^{p_2 \cdot \omega t} + i_{dn,2VF,g} + i_{dn,2VF,w} \quad (17)$$

$$i_{d,2VF} = c_{d,2VF,1} \cdot e^{p_1 \cdot \omega t} + c_{d,2VF,2} \cdot e^{p_2 \cdot \omega t} + i_{d,2VF,g} + i_{d,2VF,w} \quad (18)$$

Besides the knowledge of the different states it is very important to know, when to change the circuit states, too. Therefore in the following the transition conditions are formulated:

- freewheeling diode blocks (3VF  $\rightarrow$  3V, 2VF  $\rightarrow$  2V):

$$i_{d,3VF} \equiv i_{dn,3VF}, \quad i_{d,2VF} \equiv i_{dn,2VF} \quad (19)$$

- freewheeling diode fires (3V  $\rightarrow$  3VF, 2V  $\rightarrow$  2VF):

$$-U_0 \equiv X_d \cdot \left. \frac{di_{d,3V}(\omega t)}{d\omega t} \right|_{\omega t = \omega t_0} + R_d \cdot i_{d,3V}(\omega t_0), \quad (20)$$

$$-U_0 \equiv X_d \cdot \left. \frac{di_{d,2V}(\omega t)}{d\omega t} \right|_{\omega t = \omega t_0} + R_d \cdot i_{d,2V}(\omega t_0)$$

- thyristor blocks (3VF  $\rightarrow$  2VF, 3V  $\rightarrow$  2V):

$$i_{dn,3VF} \equiv i_{k,3V}, \quad i_{dn,3V} \equiv i_{k,3V} \quad (21)$$

- thyristor fires (2VF  $\rightarrow$  3VF, 2V  $\rightarrow$  3V):

$$i_{dn,2VF} \equiv i_{dn,3VF} \wedge i_{d,2VF} \equiv i_{d,3VF}, \quad i_{d,2V} \equiv i_{d,3V} \quad (22)$$

The last transition is automatically fulfilled all 60°, because of the periodic fire pulses of the six-pulse rectifier.

A very important angle within the calculation is the displacement angel  $\gamma$ , which describes the phase shift between the maximum of the open-circuit voltages  $u_{pR}$ , the exciting voltage, and the time, at which the firing angle  $\alpha$  for thyristor T3 starts to count. This correlation

$$\gamma = \alpha + 60^\circ \quad (23)$$

is illustrated in Fig. 12. By equations (1) and (23) a direct relation between the angle  $\gamma$ , used for the calculation, and the firing angle  $\alpha_0$ , which must be adjusted in real at the DFCL, is given.

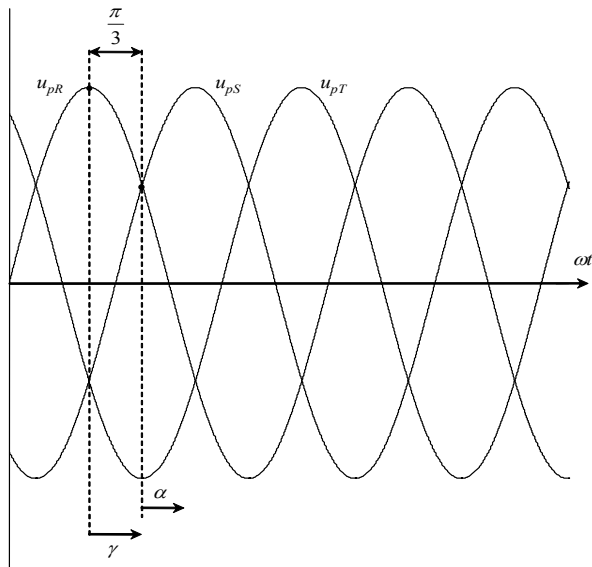


Fig. 12: Correlation between the displacement angle  $\gamma$  and the firing angle  $\alpha$

To determinate at which displacement angel  $\gamma$  or firing angle  $\alpha_0$  respectively the steady state of the DFCL with always three conductive thyristor valves is given, one has to choose a starting displacement angel  $\gamma$ . Further the associated stationary parts (Indices  $w$  (alternating) and  $g$  (d.c.)) and the eigenvalues of all state currents has to be calculated. In addition an initial value for the transient part of an arbitrary state must be chosen. Starting from this state the d.c. period is repeatedly run through in consideration of the transition conditions and the thyristor firing every 60° (see equation (22)) till all initial values of the transient current parts during the d.c. period are constant. Thereby every new d.c. period starts at  $\omega t=0$ . If all initial states are constant, the steady state for the selected displacement angle  $\gamma$  is reached. To check if at this  $\gamma$  the desired DFCL operation mode is given, one has to look, at which time condition (21) is fulfilled. If it is valid at  $\omega t=\pi/3$  the actual displacement angle  $\gamma$  is the

searched one. If equation (21) is fulfilled at a normalized time  $\omega t$  smaller than  $\pi/3$ , a greater displacement angle  $\gamma$  has to be chosen and the calculation has to be made anew. Vice versa in case of a time  $\omega t$  greater than  $\pi/3$ , a smaller displacement angle  $\gamma$  has to be taken for the new calculations.

#### 4. Results and implications for the control unit of the DFCL

In order to find out within which borders the firing angle  $\alpha_0$  can vary depending on alternating impedance ratios, two different impedance cases were investigated.

The analysed structure is the circuit diagram in Fig. 5 and its simplification in Fig. 6. In Fig. 5 the three-phase system, which is protected by the DFCL, is represented by only a resistance  $R_L$  and a reactance  $X_L=\omega L_L$ . In general the protected system could be more complex of course. During normal, faultless system operation the impedance ratio of the whole system changes permanently for example by additional or switched off loads or even by motor star-ups. These changes are taken into consideration by the change of the resistance  $R_L$  and the reactance  $X_L$ . In the simplified structure of Fig. 6 thereby the resistance  $R_k$  and the reactance  $X_k$  get other values, too. Altogether in the following the operational impedance changes within the protected system are expressed by alternating values of  $R_k$  and  $X_k$ .

For different  $R_k/X_k$ -ratios and a given limiting coil ( $R_d, X_d$ ) the calculated displacement angel  $\gamma$  or firing angle  $\alpha_0$  respectively is presented in tables 1 and 2.

Table 1. Operating area of the firing angle  $\alpha_0$  for different  $R_k/X_k$ -ratios – case 1

$R_d = 1.28 \text{ m}\Omega, X_d = 47.12 \text{ m}\Omega$					
$R_k [\text{m}\Omega]$	$X_k [\text{m}\Omega]$	$R_k/X_k$	$\gamma [^\circ]$	$\alpha_0 [^\circ]$	$\alpha'_0 [^\circ]$
1.28	12.48	0.104	110.38	20.38	80.38
1.28	9.48	0.135	107.48	17.48	77.48
1.28	6.48	0.197	102.20	12.20	72.20
1.28	3.48	0.368	89.67	-0.33	59.67
1.28	1.48	0.865	66.32	-23.68	36.32

Table 2. Operating area of the firing angle  $\alpha_0$  for different  $R_k/X_k$ -ratios – case 2

$R_d = 1.28 \text{ m}\Omega, X_d = 12.48 \text{ m}\Omega$					
$R_k [\text{m}\Omega]$	$X_k [\text{m}\Omega]$	$R_k/X_k$	$\gamma [^\circ]$	$\alpha_0 [^\circ]$	$\alpha'_0 [^\circ]$
1.28	12.48	0.104	110.43	20.43	80.43
1.28	9.48	0.135	107.54	17.54	77.54
1.28	6.48	0.197	102.26	12.26	72.26
1.28	3.48	0.368	89.68	-0.32	59.68
1.28	1.98	0.646	74.49	-15.51	44.49

All results in tables 1 and 2 are verified by models built up in the simulation tool Matlab/Simulink.

Both sample cases given in tables 1 and 2 show that the firing angle of a six-pulse thyristor rectifier is very dependent on the  $R_k/X_k$ -ratio of the three-phase system and the coil values  $R_d$  and  $X_d$  have got only little influence. This tendency can also be confirmed by other examples. A change of the system impedances can lead in both considered cases to a necessary variation of the firing angle of about  $44^\circ$ .

These results show that the permanent change of the impedances in the protected system would always require an adaptation of the firing angle  $\alpha_0$ . Of course this is possible by a fast control, but the control delay will lead to system disturbances permanently. The results of table 1 and 2 show, that it is very easy, to guarantee the desired DFCL operation mode with always three conducting thyristors, if one knows (or could well estimate) the operational borders of the system's impedances. These borders define also a maximum and a minimum firing angle  $\alpha_0$ . So the control unit of the DFCL has just to provide that between  $\alpha_{\min}$  and  $\alpha_{\max}$  always is a firing pulse on the respective thyristor (see Fig. 13). By this firing strategy with firing pulse bursts the whole operation range is covered and no automatic adaptation of the firing angle  $\alpha_0$  is necessary.

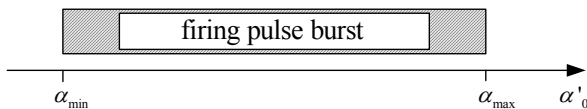


Fig. 13: Firing strategy for the thyristor pulses of a DFCL

To avoid the negative values of the firing angle  $\alpha_0$  the use of other reference voltages is recommendable. The most elegant way to realize this is to use the original firing pulses of thyristor T1 for thyristor T2, the original firing pulses of thyristor T2 for thyristor T3 and so on. By this one obtains a  $60^\circ$  phase shift and the new firing angle  $\alpha'_0$ , which is also given in tables 1 and 2. By this measure it is also easier to realize the firing pulse burst in the control unit.

## 5. Conclusion

In this paper the stationary operation mode of the DFCL in case without a fault is presented. Furthermore a numerical method is given, how to investigate the correlation of the firing angle  $\alpha_0$  with the impedance conditions of the system, which is protected by the DFCL. As a result a reasonable control strategy for the DFCL is derived, to provide always the desired operation mode of the DFCL. The results concerning the coherence between the firing angle and the impedance ratios of Fig. 6 can also contribute to the theoretical understanding of six-pulse thyristor rectifiers.

## References

[1] H. Rubenbauer, G. Herold, A Dynamic Fault Current Limiter (DFCL). *IEEE PES PowerAfrica 2007*

*Conference and Exposition Johannesburg, South Africa, July 2007.*

[2] H. Rubenbauer, G. Herold, Simulation of a Power Electronic Based Fault Current Limiter (FCL) in Case of Different Faults, *12th International Power Electronics and Motion Control Conference EPE-PEMC 2006*, 30<sup>th</sup> August–1<sup>st</sup> September 2006, Portoroz (Slovenia), Proceedings pp 550-554

[3] G. Herold, H. Rubenbauer, A. Bartmann, Calculation of a three phase fault in a network with a power electronic based Fault Current Limiter (FCL), *11th European Conference on Power Electronics and Applications*, 11.-14. September 2005, Dresden (Germany), report 652.